Polypropylene in the Melt State as a Medium for *In Situ* Synthesis of Copper Nanoparticles

Humberto Palza, Katherine Delgado, Natalia Moraga, and Sing-Hi Wang Molina
Dept. de Ingeniería Química y Biotecnología, Facultad de Ciencias Físicas y Matemáticas, Universidad de Chile, Beauchef 850, Santiago, Chile

DOI 10.1002/aic.14549
Published online July 21, 2014 in Wiley Online Library (wileyonlinelibrary.com)

Copper nanoparticles were in situ synthesized into a polypropylene matrix in the melt state. Three different routes were studied depending on the method used for the addition of a copper salt: (1) directly as powder; (2) dissolved in water; and (3) dissolved in water with a reducing agent. The first route produced microcrystal, whereas the second route allowed the synthesis of nanoparticles (~20 nm) homogeneously dispersed in the polymer matrix. By changing the concentration of the reducing agent in the copper solution (third route), a control of the copper structure in the polymer was possible and salt-based or metal/oxide nanoparticles could be obtained. All these composites were able to release copper ions depending on the characteristic of the nanoparticles present in the polymer. Noteworthy, the resulting polymer/copper composites displayed strong antimicrobial behavior against Escherichia coli. © 2014 American Institute of Chemical Engineers *AIChE J*, 60: 3406–3411, 2014

Keywords: biomaterials, composite materials, nanotechnology, polymer processing

Introduction

Synthesis of nanoparticles is a relevant topic due to the extraordinary properties that can be found at the nanoscale such as electronic, optical, and mechanical, among others. These properties are related with new physical/chemical phenomena that do not exist in materials with larger sizes.[1] Polymer science can merge with this extraordinary field by two general approaches: (1) polymer as a template or as an assistant for the preparation of nanoparticles, generally a hybrid material[1–3]; and (2) polymer as a matrix where the nanoparticles are embedded producing a nanocomposite.[4,5] The first approach allows the synthesis of more stable particles reducing its self-aggregation and increasing its stability.[1,6] For instance, because of the large decrease in its surface energy, nanoparticles coated by a polymer shell are considerably more stable against aggregation than bare particles.[6] The second approach allows the simplest way to take advantage of the extraordinary properties of nanoparticles at macroscale. In fact, one of the first commercial patents related with carbon nanotubes was a polymer composite avoiding the manipulation of nanoparticles by just mixing it.[7] Therefore, the *in situ* preparation of nanoparticles into a polymer matrix obtaining a macroscale composite, combining the aforementioned two approaches, seems to be a good route to develop novel materials. Polymer/nanoparticle composites prepared by this route have been largely studied for hydrogels or other functional polymers,[8–13] such as thin film systems.[14–16] However, in nonpolar thermoplastic matrices, such as polyolefins, the *in situ* synthesis of nanoparticles has been scarce.[17,18]

From the different kinds of nanoparticles, those having antimicrobial behavior are highlighted as they can be added into a polymer matrix producing novel biocide materials. Nowadays, antimicrobial polymeric materials are largely demanded as they could avoid the spread of hospital-acquired infections responsible of prolonged hospital stay, increased morbidity and mortality for patients, and being responsible of around 5–10% of all hospitalizations.[19,20] In this context, polymer composites based on metal nanoparticles displaying strong antibacterial are highlighted.[21–26] Nanoparticles are more efficient than microparticles due to the high specific area increasing the release of metal ions.[21] From the different metals used, copper emerges as an outstanding materials as it has been used for centuries as bactericide, fungicide, and also as antifouling agent.[27] Unlike other biocide metals, such as silver, copper is an essential micronutrient to human with low toxicity levels.[28] Moreover, human skin has low sensitivity to copper allowing its use for anti-inflammatory and healing treatments,[29] and for intrauterine devices. As antimicrobial nanosize agents, copper nanoparticles have antimicrobial specificity against *Bacillus subtilis* and *Escherichia coli* bacteria unlike other nanoparticles.[30]

Antimicrobial thermoplastic polymers based on metal nanoparticles had been produced by several methodologies such as melt mixing where particles are embedded homogeneously in the matrix[21,22,24–26] or surface coatings.[23] All these methodologies used metal/oxide nanoparticles synthesized *ex situ* before its incorporation in the polymer matrix. The goal of the present manuscript is to use a thermoplastic polymer matrix in the melt state as a medium for the

Correspondence concerning this article should be addressed to H. Palza at hpalza@ing.uchile.cl.

synthesis of copper nanoparticles. By changing the method used to add the copper reagents, a control of the structure of the nanoparticles was obtained. Moreover, using this methodology, novel antibacterial polypropylene (PP) composites were produced as shown in this contribution, with strong application in biomedical devices.

The methodology presented is based on the behavior of a water drop in contact with a hot surface above the saturation temperature (polymer melt in our case) as we assume that water does not dissolve in PP. The first process to be considered relates with the physical impact between the drop and a dry surface producing stick to the surface, bounce off, or splash and split into smaller droplets.[31,32] The second process relates with the boiling process generated by the hot surface producing convective motions activated by the heat flux through the liquid and the liquid–vapor phase transition.[32] Both processes are related as the process of drop break-up is enhanced by boiling initiated at the contact points between the liquid and the hot material.[32] In our case, the interface is relevant as a vapor layer between the drop and the hot surface is formed in which the concentration of the dissolved salt is increased.[33] The considerable temperature gradient in this layer leads to further supersaturation of the solution and crystal nuclei precipitate.[33] In this process is expected the formation of nanocrystal. Therefore, we assume that the original milimetric water drop with the copper dissolved becomes much smaller and well dispersed in contact with the polymer melt and its high shear stresses. Afterward and due to the high temperature of the media, a thin vapor interface will be generated between the polymer and the drop where copper nanocrystals can be formed.

Experimental

A commercial isotactic PP in the melt state (PH0320 from Petroquim S.A. Chile, with a melt flow index of 3,3 g/10 min ASTMS D-1238/95), was used as the reaction medium. For the reactions, a Brabender plasticorder melt mixer was used at 190°C, 110 RPM, and 10 min, under nitrogen atmosphere. The copper nanoparticle precursor was copper(II) acetate monohydrate ($Cu(CH_3COO)_2H_2O$) from May & Baker. Typically, 30 g of PP was added to the melt mixer at 190°C and 30 RPM. When all the polymer was melt, the precursor was added and afterward the speed of the screw was increased to 110 RPM and the system was allowed to react 10 min. All the composites prepared have 10 w/w % of copper. Three different routes were tested: (1) the direct addition of the precursor (powder) into the polymer in the melt state (R1); (2) the addition (dropwise) into the polymer of a water solution having the desired amount of precursor (R2); and (3) the addition (dropwise) into the polymer of a water solution having the desired amount of precursor and sodium formaldehyde sulfoxylate (SBF) as a reducing agent (R3). The composites were press molded at 190°C at 50 bar for 5 min and cooled under pressure by flushing the press with cold water, resulting a film of about 1-mm thick.

The release of cupric ions was measured using a UV-Visible Agilent (Model 8453) spectrophotometer. The ions concentration of 3 mL of samples solutions were determined by adding 1 mL of 10% hydroxylamine hydrochloride solution, 1 mL de sodium acetate-acetic buffer (pH = 4.5), and 1 mL of 1.92×10^{-3} M neocuproine (cooper reagent). The neocuproine was used to form a yellow chelate with the cupric ions. The size of nanoparticles and their dispersion into the polymer was determined by transmission electron microscopy using a Phillips Model Tecnai 12 Biotwin operated at 80 kV. Samples of polymer were cut to 70 nm of thickness using a Reichert–Jung (Leica) Ultracut ultra microtome with a diamond knife and put onto a 300 mesh copper grid. Wide angle x-ray diffraction analysis was performed using a Siemens D-5000 diffractometer with CuKα = 1.54 Å and a step scan of 0.02° at room temperature. To estimate the size of the crystals from x-ray analysis, the MDI Jade 6.5 software was used allowing the application of the Scherrer equation. In this way, the size of the ordered (crystalline) domains was measured. The crystallite shape factor used was 0.9, applied for spherical particles.

The bacteria were grown overnight in Lysogeny Broth (LB)–Luria at 37°C for the antimicrobial tests. LB is a bacterial culture medium used for the growth of bacteria, its standard recipe for 10^{-3} m^3 is Tryptone (10 g), Yeast Extract (5 g), and NaCl (0.5 g). Afterward, the bacterial count was standardized to $\sim 10^8$ CFU/mL by measuring their optical density and maintained at 37°C for 2 h to avoid the lag-phase of the kinetic bacterial growth. The initial concentration of bacteria was determined by the solid agar plate method. An aliquot of 40×10^{-9} m^3 of the bacteria broth was poured into the sample surface and covered with a glass during a specific time ranging from 30 to 360 min at 37°C. After the time was elapsed, the samples were thoroughly washed with a solution of 0.88 wt % of NaCl and 1 wt % of Tween 80 to remove the survival bacteria from the surface. From this solution, an aliquot of 40 μL was extracted, transferred onto a nutrient agar, and incubated for 57.6×10^4 s at 37°C before colonies were counted. All the experiments were repeated at least twice on different days. The samples, tools, glass materials, and wells were sterilized using an Orthmann autoclave for 1.2×10^3 s at 1 bar and 140°C before any experiment.

Results

X-ray diffractions

Figure 1 shows the x-ray diffraction patterns from PP composites produced by R1 (precursor added as powder) and R2 (precursor added previously dissolved in water) routes. From this figure is clear that both routes mainly produced copper acetate tetragonal crystals embedded in the polymer matrix as the main peaks were found at 11.3, 12.0, 14.8, 17.9, and 23.5°. The precursor is copper(II) acetate monohydrated that is dehydrated between 125 and 225°C producing copper(II) acetate as observed in Figure 1.[33] Therefore, the temperature of the mixer (190°C) was high enough to dehydrate the precursor. However, despite the reaction was performed under nitrogen atmosphere and at a temperature below those reported for decomposition of the precursor (between 220 and 325°C), diffraction peaks related with copper oxides were further observed.[34] In particular, tenorite (CuO) and cuprite (Cu_2O) crystalline phases with peaks at 35.5 and 38.78°, and 36.4 and 42.5°, respectively, appear. R2 route produced a higher amount of these copper oxides, in particular tenorite. The appearance of these oxides can be related with the increased local temperature in the polymer bulk because of the high frictional forces produced by the macromolecules in the melt mixer. If high shear stresses are applied to a polymer, the heat generated by the viscous dissipation leads to a temperature rise of the melt.[35] The presence

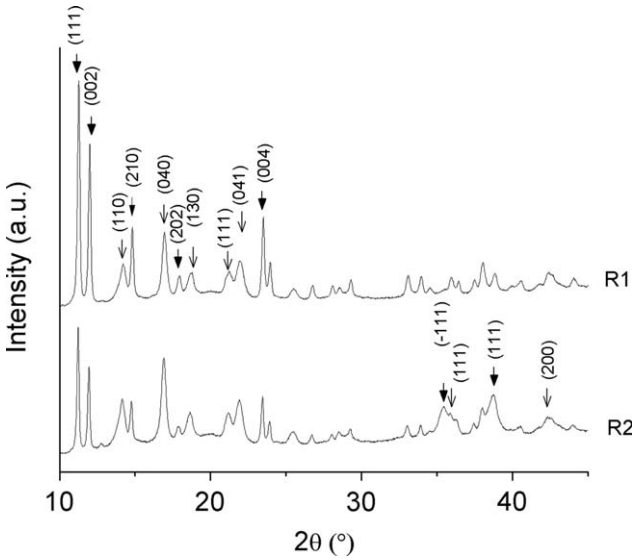

Figure 1. X-ray diffractions of PP/copper composites prepared by R1 (up-curve) and R2 (down-curve) routes.

Up-curve: Close arrows and open arrows represent the peaks associated with copper acetate and PP crystals, respectively. Down-curve: Close arrow and open arrow represent the peaks associated with CuO tenorite and Cu_2O cuprite crystals, respectively.

of oxygen traces further explains the presence of copper oxides as secondary products in our methodology.

On the basis of aforementioned, we can summarize the different chemical reactions involved. Initially, the precursor was dehydrated between 125 and 225°C inside the melt mixer forming the anhydride[34]

$$Cu_2(CH_3COO)_4 * H_2O \rightarrow 2Cu(CH_3COO)_2 + 2H_2O \quad (1)$$

Then, a thermal decomposition occurred involving several simultaneous reactions where copper oxide and metallic copper were obtained from the 200°C[36]

$$Cu(CH_3COO)_2 \rightarrow CuO + CH_3CHO + H_2O + C + CO_2 \quad (2)$$

$$CuO + CH_3CHO \rightarrow Cu_2O + CO_2 \quad (3)$$

$$CuO + CO \rightarrow Cu + CO_2 \quad (4)$$

$$C + 2CuO \rightarrow Cu + CO_2 \quad (5)$$

$$6n\,Cu(CH_3COO)_2 + \frac{1}{2}O_2 \rightarrow Cu + Cu_2O + 3n\ \text{volatiles} \quad (6)$$

$$Cu + \frac{1}{2}O_2 \rightarrow CuO \quad (7)$$

$$2Cu + \frac{1}{2}O_2 \rightarrow Cu_2O \quad (8)$$

$$Cu_2O + \frac{1}{2}O_2 \rightarrow CuO \quad (9)$$

Our results showed that the thermal decomposition of copper acetate by R1 or R2 route was not complete displaying a low yield.

Two variables were analyzed trying to optimize the yield of the system toward copper oxide particles: mixing time and amount of precursor (copper acetate) added to the melt mixer. The effect of time was performed comparing the results obtained after 10 and 30 min of mixing. However, changes on the characteristic diffraction peaks of the composites were not observed allowing the conclusion that mixing time is not a relevant variable (results not shown). Figure 2 otherwise presents the results from samples prepared by R2 route using different amounts of copper acetate, from 1 to 10 wt % of copper. At low amount of precursor, the diffraction peaks associated with the polymer matrix were mainly observed (dilution effect). By increasing the amount of precursor, the same peaks related with the salt and the copper oxides were mainly observed with the same relative intensity showing that the amount of copper acetate was not a relevant variable in the yield of the reactions involved.

When R3 route is used, meaning that the copper salt is dissolved in water with a reducing agent (SBF) previous to the addition into the polymer, drastic changes were observed depending on the precursor/SBF molar ratio, as displayed in Figure 3. The main consequence of the presence of SBF was the absence of diffractions peaks associated with either copper acetate or the reducing agent itself, showing a high reaction yield toward copper metal/oxide particles by R3 route. SBF has been previously tested for preparation of silver, gold, and copper nanoparticles, as its mild reducing nature avoids both fast reaction kinetics and the formation of oxides.[37] At the highest precursor/SBF ratio the composite presented diffraction peaks at 36.7, 42.5, 61.5, and 73.5° meaning Cu_2O cuprite particles. At a molar ratio equal to 1, the diffraction pattern changed with peaks at 43.4, 50.6, 74.2° meaning copper metal particles. When the ratio is equal to 2.0, both copper oxide and copper metal particles appeared. Therefore, by changing the amount of SBF, a control on the kind of copper particles produced into the PP in the melt state was obtained: from copper acetate to metal copper. We further analyzed the effect of adding different amounts of copper, from 1 to 10 wt %, at a molar ratio equal to 1. Similar to the observed for composites prepared by R2 route (Figure 2), changes in the relative intensity of the diffraction peaks were not observed and copper metal was the main compound produced (results not shown).

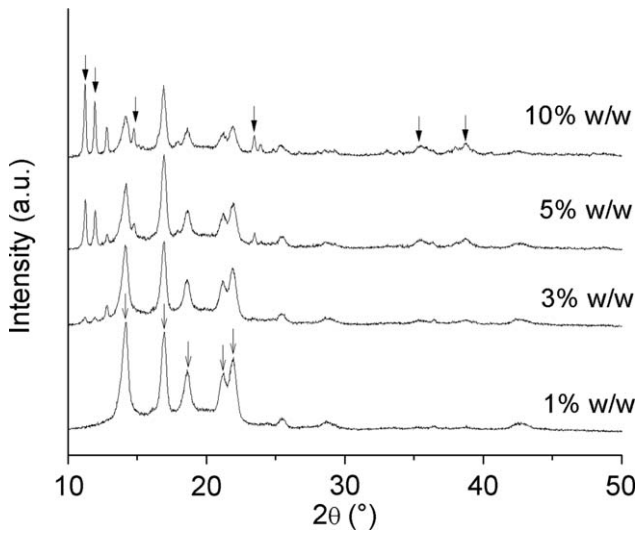

Figure 2. X-ray diffractions of PP/copper composites prepared by R2 route using different amounts of copper acetate, from 1 to 10 wt % of copper.

Close arrows represent the peaks associated with copper acetate, Cu_2O, and Cu crystals, and open arrows represent the peaks of PP crystals.

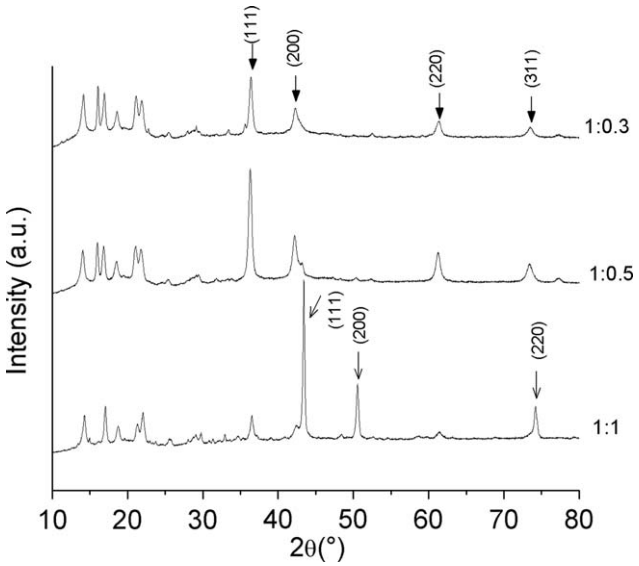

Figure 3. X-ray diffractions of PP/copper composites prepared by R3 route at different precursor/SBF molar ratios.

Close arrows and open arrows represent the peaks associated with Cu_2O and Cu crystals, respectively.

The reactions involved using R3 are due to the presence of the sodium formaldehyde sulfoxylate (SBF) acting as reducing agent for the copper ions by means of the ion sulfoxylate (HSO_2^-) according to the next reactions[38,39]

$$HOCH_2SO_2^- + H_2O \leftrightarrow HSO_2^- + CH_2(OH)_2 \quad (10)$$

$$HOCH_2SO_2^- \leftrightarrow HSO_2^- + CH_2O \quad (11)$$

Therefore, Cu^{2+} ions obtained from either the thermal decomposition or the water dissolution of copper acetate can be reduced explaining the results from Figure 3.

TEM characterization

Despite R1 and R2 routes displayed the same x-ray diffraction patterns (Figure 1), the morphology of the resulting particles embedded in the composites was largely affected as observed by TEM images (Figures 4 and 5). By adding copper salt powder to the polymer (R1), well dispersed hexagonal crystals were mainly observed into the matrix (Figure 4) with homogeneous sizes (~300 nm). These crystals can be related with copper acetate crystals as observed by x-ray diffractions. Together with these hexagonal crystals, smaller structures were visualized associated with copper oxide particles found in this sample (Figure 1). By following R2 route

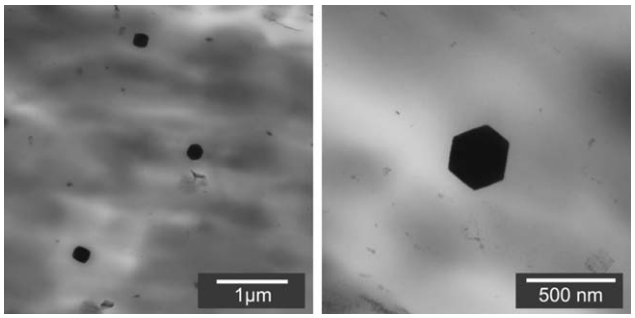

Figure 4. Transmission electron micrographs of PP/copper composites prepared by R1 route.

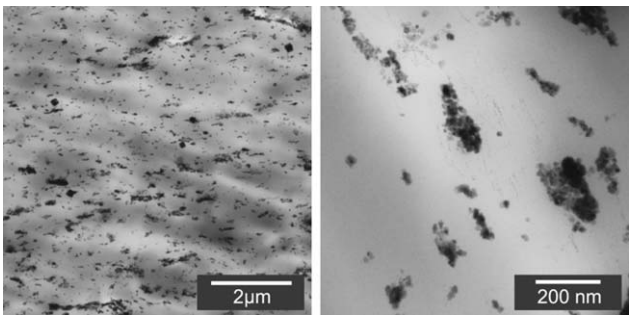

Figure 5. Transmission electron micrographs of PP/copper composites prepared by R2 route.

otherwise, a different morphology was obtained in the composite (Figure 5) as nanoparticles around ~20 nm forming well dispersed agglomerates of ~150 nm were mainly observed. These nanostructures could be a mix of the different compounds observed in Figure 1: copper acetate and copper oxide particles. Moreover, the smallest particles observed in Figure 5 were similar to the small structures observed in Figure 4. Composites obtained by R3 route also produce copper nanoparticles with sizes between 50 and 100 nm, depending on the molar ratio of the reagents (see Table 1 and Figure 6). These particles were highly agglomerated in the polymer matrix forming secondary structures with sizes of ~500 nm (precursor/SBF ratio equal to 1). This morphology was not affected by the amount of SBF as composites prepared with molar ratios equal to either 2.0 (left side of Figure 6) or 1.0 (right side of Figure 6) displayed the same structures. This kind of agglomeration seems to be related with the nature of the nanoparticles as it was also observed in similar PP/metal copper composites although using commercial nanoparticles.[26] To further confirm the nanostructures obtained, the Scherrer equation was used allowing the estimation of the size of the ordered (crystalline) domains from x-ray diffractions.[40] This equation was not used for composites prepared by R1 route as is valid for grains smaller than 0.1 μm. The results displayed in Table 1 confirmed the TEM analysis as crystals in the nanoscale were measured by this equation with values as similar as those coming from the images.

TEM results confirmed our strategy to synthesize copper nanostructures based on the phenomenology behind the drop impact in a hot insoluble media. In this case, the original drop decreases its size by the physical impact on the surface and the high shear stresses in the media becoming homogeneously dispersed in the media. Afterward, a vapor layer interface is formed on the surface of the small drops due to the high temperature of the media as compared with the saturation temperature of water.[31–33] In this interface, the

Table 1. Effect of the Route Used on the Particle Size Synthesized in the Polymer Melt as Measured by the Scherrer Equation and TEM Analysis

Reaction	Particle	Size by Scherrer Equation (nm)	Size by TEM Images (nm)
R1	Copper acetate	Not applicable	~300
R2	Tenorite (CuO)	12 ± 9	27 ± 8
R2	Cuprite (Cu_2O)	22 ± 1	27 ± 8
R3(1:0.5)	Cuprite Cu_2O	20 ± 0.2	112 ± 30
R3(1:0.3)	Copper (Cu)	47 ± 0.6	45 ± 4

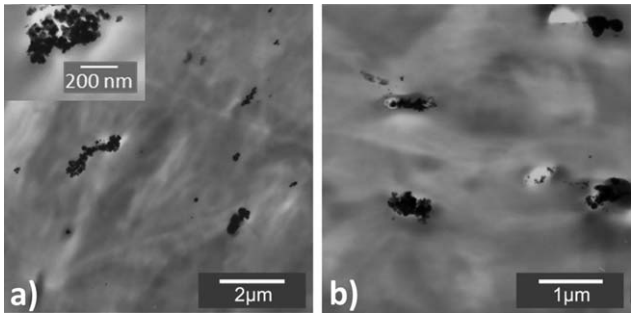

Figure 6. Transmission electron micrographs of PP/copper composites prepared by R3 route: (a) 1/0.5 and (b) 1/1 molar ratio of copper acetate and SBF.

copper salt concentration is oversaturated allowing the nanocrystal precipitation.[31–33]

Copper ion release and antimicrobial tests

Although several mechanisms can explain the antimicrobial behavior of polymer/metal composites, the release of metal ions is one of the main processes involved.[23,26] Figure 7 displays the copper ion release from the different composites showing the strong effect of the kind of particle on its behavior. Composites having mostly copper acetate crystals salts (R1 and R2) were able to release 10 times more ions than both metal and oxide copper particles. Moreover, the sample having large crystal salts (R1) showed larger ion release than composite with nanocrystal salts and copper oxides (R2). It is clear that the dissolution of a water soluble salt (copper acetate) should be much faster than the corrosion processes of copper particles, either metal or oxide, where several mechanisms occur and the diffusion of oxygen is required.[41] Based on these results showing the release of metal ions from the different composites, an antimicrobial behavior should be expected. Noteworthy, independent of the route used to prepare the composites, all these samples were able to eliminate more than 99.9% of *E. coli* after 4 h of contact as displayed in Figure 8. The high toxicity of copper can be associated with several factors related with the presence of its ions interacting with different functional

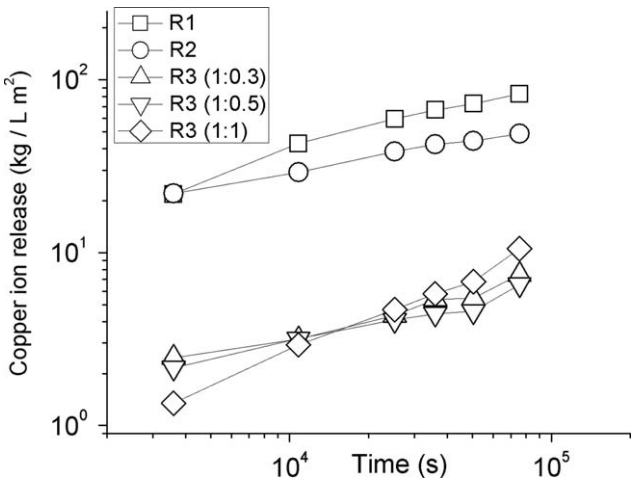

Figure 7. Copper ion release from the different PP/copper composites prepared by R1, R2, and R3 routes.

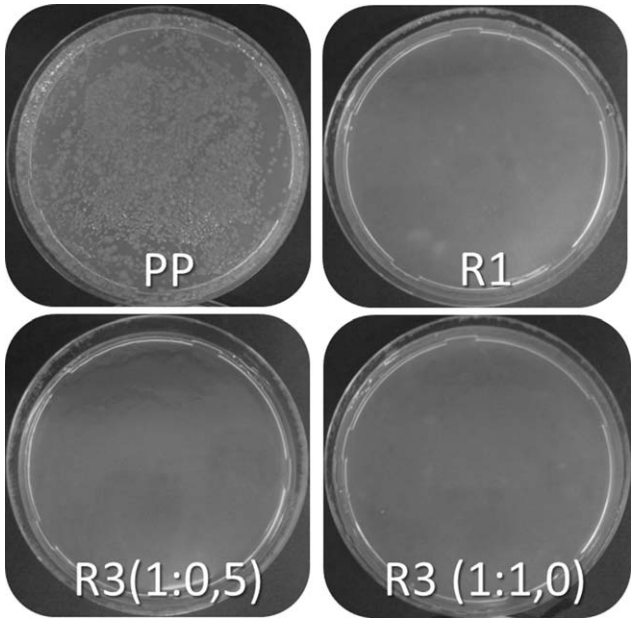

Figure 8. Pictures of *E. coli* living colonies after 4 h of contact on the representative samples.

groups present in the microorganism.[27] Copper ions can interact directly with the cell membrane or increase the concentration of reactive oxygen species overwhelming the natural antioxidant defense of the microorganism.[42] Independent of the mechanism, copper ion is the main active agent killing bacteria confirming the relevance of the metal ion release from the polymer composite.

Conclusions

The *in situ* synthesis of copper nanoparticles into a PP matrix in the melt state was carried out allowing the development of antimicrobial polymer composites. Three different routes were studied depending on the method used for the addition of a copper salt: (1) directly as powder; (2) dissolved in water; and (3) dissolved in water with a reducing agent. Depending on the route used, copper nanoparticles were produced into the PP matrix. The nature of the nanoparticles can be tailored by the presence of a reducing agent and either salt-based or oxide/metal copper particles were synthesized. Noteworthy, the release of copper ions depended on the nature of the copper particles embedded in the PP matrix and composites having salts release 10 times more ions than those having metal/oxide particles. Composites produced by this method were able to kill *E. coli* confirming the antimicrobial behavior of the materials produced.

Acknowledgment

The authors gratefully acknowledge the financial support of CONICYT, project FONDECYT 1110078.

Literature Cited

1. Pomogailo AD, Kestelman VN. *Metalpolymer Nanocomposites*. Germany: Springer, 2005.
2. Rao T, Dong XH, Katzenmeyer BC, Wesdemiotis C, Chenga SZD, Becker ML. High-fidelity fabrication of Au–polymer Janus nanoparticles using a solution template approach. *Soft Matter*. 2012;8:2965–2971.
3. Ethirajan A, Landfester K. Functional hybrid materials with polymer nanoparticles as templates. *Chem Eur J*. 2010;16:9398–9412.

4. Ray S, Okamoto M. Polymer/layered silicate nanocomposite: a review from preparation to processing. *Prog Polym Sci*. 2003;28: 1539–1641.
5. Paul DR, Robeson LM. Polymer nanotechnology: nanocomposites. *Polymer*. 2008;49:3187–3204.
6. Rozenberg BA, Tenne R. Polymer-assisted fabrication of nanoparticles and nanocomposites. *Prog Polym Sci*. 2008;33:40–112.
7. Moniruzzaman M, Winey KI. Polymer nanocomposites containing carbon nanotubes. *Macromolecules*. 2006;39:5194–5205.
8. Ramesh GV, Porel S, Radhakrishnan TP. Polymer thin films embedded with in situ grown metal nanoparticles. *Chem Soc Rev*. 2009;38: 2646–2656.
9. Feldgitscher C, Ivanovici S, Kickelbick G. Versatile Hybrid Polymers as Matrices for Nanoparticle Preparation. *MRS Proc*. 2007; 1007:s12.
10. Wang DY, Song YP, Wang JS, Ge XG, Wang YZ, Stec AA, Hull TR. Double in situ approach for the preparation of polymer nanocomposite with multi-functionality. *Nanoscale Res Lett*. 2009;4:303–306.
11. RangaReddy P, MohanaRaju K, SubbaramiReddy N. A review on polymer nanocomposites: monometallic and bimetallic nanoparticles for biomedical, optical and engineering applications. *Chem Sci Rev Lett*. 2013;1:228–235.
12. Zhang Z, Han M. One-step preparation of size-selected and well-dispersed silver nanocrystals in polyacrylonitrile by simultaneous reduction and polymerization. *J Mater Chem*. 2003;13:641–643.
13. Ruiz P, Muñoz M, Macanas J, Muraviev DN. Intermatrix synthesis of polymer-copper nanocomposites with tunable parameters by using copper comproportionation reaction. *Chem Mater*. 2010;22:6616–6623.
14. Porel S, Singh S, Harsha SS, Rao DN, Radhakrishnan TP. Nanoparticle-embedded polymer: in situ synthesis, free-standing films with highly monodisperse silver nanoparticles and optical limiting. *Chem Mater*. 2005;17:9–15.
15. Korchev AS, Bozack MJ, Slaten BL, Mills G. Polymer-initiated photogeneration of silver nanoparticles in SPEEK/PVA films: direct metal photopatterning. *J Am Chem Soc*. 2004;126:10–11.
16. Rifai S, Breen CA, Solis DJ, Swager TM. Facile in situ silver nanoparticle formation in insulating porous polymer matrices. *Chem Mater*. 2006;18:21–25.
17. Stará H, Starý Z, Münstedt H. Silver nanoparticles in blends of a polyethylene and superabsorbent polymer: morphology and silver ion release. *Macromol Mater Eng*. 2011;296:423–427.
18. Bahloul W, Oddes O, Bounor-Legare V, Melis F, Cassagnau P, Vergnes B. Reactive extrusion processing of polypropylene/TiO2 nanocomposites by in situ synthesis of the nanofillers: experiments and modeling. *AIChE J*. 2011;57:2174–2184.
19. Leth RA, Møller JK. Surveillance of hospital-acquired infections based on electronic hospital registries. *J Hosp Infect*. 2006;62:71–79.
20. Balkhya HH, Cunninghama G, Chewa FK, Francis C, Nakhli DJA, Almuneef AMA, Memish ZA. Hospital- and community-acquired infections: a point prevalence and risk factors survey in a tertiary care center in Saudi Arabia. *Int J Infect Dis*. 2006;10:326–333.
21. Damm C, Münstedt H, Rösch A. The antimicrobial efficacy of polyamide 6/silver-nano- and microcomposites. *Mater Chem Phys*. 2008; 108:61–66.
22. Radheshkumar C, Münstedt H. Antimicrobial polymers from polypropylene/silver composites–Ag+ release measured by anode stripping voltammetry. *React Funct Polym*. 2006;66:780.
23. Cioffi N, Torsi L, Ditarantano N, Tantalillo G, Ghibelli L, Sabbatini L, Bleve-Zacheo T, D'Alessio M, Zambonin PG, Traversa E. Copper nanoparticle/polymer composites with antifungal and bacteriostatic properties. *Chem Mater*. 2005;17:5255–5262.
24. Cai S, Xia X, Xie C. Corrosion behaviour of copper/LDPE nanocomposites in simulated uterine solution. *Biomaterials*. 2005;26: 2671–2676.
25. Palza H, Gutiérrez S, Delgado K, Salazar O, Fuenzalida V, Avila J, Figueroa G, Quijada R. Toward tailor-made biocide materials based on polypropylene/copper nanoparticles. *Macromol Rapid Commun*. 2010;31:563–567.
26. Delgado K, Quijada R, Palma R, Palza H. Polypropylene with embedded copper metal or copper oxide nanoparticles as a novel plastic antimicrobial agent. *Lett Appl Microbiol*. 2011;53:50–54.
27. Borkow G, Gabbay J. Copper as a biocidal tool. *Curr Med Chem*. 2005;12:2163–2175.
28. Massaro EJ. *Handbook of Copper Pharmacology and Toxicology*. Totowa, NJ: Humana Press, 2002.
29. Dreher F, Harrison BJ, Hostýnek JJ, Maibach HI, Michels HT, Milanino R, et al. In: Hostýnek JJ, Maibach HI, Editors. Copper and Skin. New York, Londres: Informa Healthcare USA Inc., 2006:1–289.
30. Yoon K, Byeon JH, Park J, Hwang J. Susceptibility constants of Escherichia coli and Bacillus Subtilis to silver and copper nanoparticles. *Sci Total Environ*. 2007;373:572–575.
31. Rein M. Phenomena of liquid drop impact on solid and liquid surfaces. *Fluid Dyn Res*. 1993;12:61–93.
32. Bertola V. Drop impact on a hot surface: effect of a polymer additive. *Exp Fluids*. 2004;37:653–664.
33. Malayeri MR, Müller-Steinhagen H, Bartlett TH. Fouling of tube bundles under pool boiling conditions. *Chem Eng Sci*. 2005;60: 1503–1513.
34. Bellini JV, Machado R, Morelli MR, Kiminami RHGA. Thermal, structural and morphological characterisation of freeze-dried copper(II) acetate monohydrate and its solid decomposition products. *Mater Res*. 2002;5:453–457.
35. Daryanani R, Janeschitz-Kriegl H, van Donselaar R, van Dam J. A calorimetric measurement of frictional heat in capillary rheometry of polymer melts. *Rheol Acta*. 1973;12:19–24.
36. Malowska J, Baranowska A. Kinetic parameters of the thermal decomposition of Cu (II) and Zn (II) salts of carboxylic acids. *J Therm Anal*. 1984;29:309–315.
37. Khanna PK, Gaikwad S, Adhyapak PV, Singh N, Marimuthu R. Synthesis and characterization of copper nanoparticles. *Mater Lett*. 2007;61:4711–4714.
38. Makarov S. Recent trends in the chemistry of sulfur-containing reducing agents. *Russ Chem Rev*. 2001;70:885–895.
39. Terskaya I, Budanov V, Makarov S, Ermolina L. Electroless nickel and copper plating of carbon fibers with the use of sulfur-containing reducing agents. *Russ J Appl Chem*. 2004;77:236–240.
40. Cullity BD, Stock SR. Elements of X-Ray Diffraction, 3rd ed. New Jersey, Prentice-Hall Inc., 2001.
41. Xia X, Xie C, Cai S, Yang Z, Yang X. Corrosion characteristics of copper microparticles and copper nanoparticles in distilled water. *Corros Sci*. 2006;48:3924–3932.
42. Gunawan C, Teoh WY, Marquis CP, Amal R. Cytotoxic origin of copper oxide nanoparticles: comparative studies with micrón-sized particles, leachate, and metal salts. *ACS Nano*. 2011;5:7214–7225.

Manuscript received Feb. 3, 2014, and revision received June 26, 2014.